JOURNAL OF GUIDANCE, CONTROL, AND DYNAMICS
Vol. 43, No. 11, November 2020

Engineering Notes

Optimal Tuning of Adaptive Augmenting Controller for Launch Vehicles in Atmospheric Flight

Domenico Trotta,* Alessandro Zavoli,† and Guido De Matteis‡
University of Rome "La Sapienza", 00184 Rome, Italy
and
Agostino Neri§
ESA, I-00044 Frascati, Italy

https://doi.org/10.2514/1.G005352

I. Introduction

A NOVEL tuning methodology for the adaptive augmenting control (AAC) component of a launch vehicle (LV) flight control system (FCS) is presented in this Note. AAC has been developed in the framework of the Space Launch System (SLS) program [1], which is the upcoming LV under development by NASA.

FCS design for LVs in atmospheric flight is a challenging task because the vehicle experiences rapidly changing inertial and aeropropulsive characteristics, interaction between low- and high-frequency dynamics due to the slender shape, inherent aerodynamic instability, and high aerodynamic loads. Also, control authority is limited to the gimbal deflection of nonthrottleable engines whose angular range is constrained to a few degrees.

Classical control systems, such as gain-scheduled proportional–integral–derivative (PID) controllers complemented by linear bending filters to suppress control interaction with vehicle flexibility, are usually able to meet basic command tracking requirements and satisfy stability and performance criteria for flight certification. However, effective design methodologies are demanded for risk reduction with respect to possible loss of performance due to model uncertainties, off-nominal flight conditions, and unexpected environmental disturbances. Furthermore, FCS robustness could be further exploited as a means for reducing the burden of recurrent activities of mission integration and flight program software finalization, including gain tuning with the related extensive validation and verification, because payload mass, target injection orbit, or launch conditions are varied for each launch.

Among several advanced algorithms referenced in the literature, the AAC has been proposed in order to retain the functionality and proven record of success of classically designed linear control systems while consistently and predictably improving their performance and robustness in expanded flight and/or uncertainty parameter envelopes [2,3]. AAC adjusts the action of a baseline PID-type controller (BC) by means of a forward loop gain multiplicative adaptive law that, basically, online modulates BC output either to minimize the error with respect to a reference model or to limit undesirable high-frequency response in the control path. Specific adaption limits are enforced to preserve BC stability margins.

A number of papers report on the advantages of AAC architecture in SLS FCS with respect to the three design objectives of 1) minimal adaptation, 2) improved performance, and 3) loss of vehicle (LOV) prevention [2–4]. AAC stability has been extensively and exhaustively investigated by a number of techniques [2,5,6], including classical frequency-domain stability analysis, Lyapunov-based stability analysis, generalized gain margins analysis, time-domain stability margin assessment, and Monte Carlo simulations with expanded dispersion. In this broad assessment perspective, which also leads to some recommendations on AAC parameter tuning, it is apparent that AAC performance objectives are met for LV operations in off-nominal conditions.

In recent times, application of the AAC architecture to the European Vettore Europeo di Generazione Avanzata (VEGA) LV in the atmospheric flight phase has been investigated, with the main purpose of improving FCS stability and performance robustness characteristics as well as to reduce the effort dedicated to the processes of preflight (re) tuning and validation. In Ref. [7], the adaptive augmentation has been applied to a BC for pitch and yaw axes designed using the structured H_∞ control technique. Again, the AAC prevents LOVs and improves BC performance, but the complexity of the adaptive law tuning process in the absence of a specific design methodology and analysis tools is remarked on as a drawback of the approach. Opportunities and limitations of AAC architecture have been also investigated in Ref. [8], with particular reference to the topics of tuning and FCS robustness enhancement.

One may conclude that, although extended capabilities of AAC architecture over flight-certified LV BCs have been demonstrated, a sound method for quantifying the benefits of the nonlinear adaptive augmentation is still to be devised. It is also apparent that selection of appropriate values of AAC parameters, where different elements (that is, reference model, logistic gain, spectral damper, and leakage) act concurrently and independently to modulate the multiplicative forward gain [4], is far from trivial. In this respect, suitability of heuristic trial-and-error tuning procedures is debatable because assessment of expected improvement of baseline FCS calls for extensive and time-consuming verification and validation activities, where stability and performance targets and criteria are not clearly established.

The rationale for the present study stems from recognition that AAC potentiality can be fully exploited provided that an effective and reliable tuning procedure is introduced. To this end, a methodology for AAC parameter tuning is presented where a robust design optimization (RDO) problem [9] is formulated, and the goal is to maximize a statistical metric that describes FCS performance measured over a set of representative simulations of LV flight. In more detail, adaptive law parameters are tuned with the aim of minimizing attitude error and traversal aerodynamic loads. In so doing, the occurrence of LOV events may be reduced [2].

In the first approach, the performance index J_{MC} is determined by Monte Carlo (MC) simulations. Albeit effective, this procedure is computationally expensive since each evaluation of J_{MC} requires a large number of runs, with model parameters suitably scattered. Moreover, J_{MC} is noisy due to the inherent randomness of the MC-based procedure, which penalizes the efficiency of optimization method. The second tuning method considers that, in marginal stability conditions, model-reference error and spectral damper outputs have major impact on the multiplicative gain variation. Therefore, adaptation law is optimized with respect to two worst-case conditions where, respectively, the low- and high-frequency gain margins of the open-loop LV model

Received 24 April 2020; revision received 9 July 2020; accepted for publication 9 July 2020; published online Open Access 13 August 2020.

*Ph.D. Student, Department of Mechanical and Aerospace Engineering, Via Eudossiana 18; domenico.trotta@uniroma1.it.

†Research Fellow, Department of Mechanical and Aerospace Engineering, Via Eudossiana 18; alessandro.zavoli@uniroma1.it.

‡Professor, Department of Mechanical and Aerospace Engineering, Via Eudossiana 18; guido.dematteis@uniroma1.it.

§Head of VEGA-C Launcher System Integration and Launch System Synthesis Office, VEGA Integrated Project Team, European Space Research Institute, Largo Galileo Galilei, 1; agostino.neri@esa.int.

used for FCS design are zero as a result of system parameter variations. The RDO problem is thus formulated as a min-max[¶] optimization, where the goal is to evaluate the AAC gains that maximize the worst-case performance across the corner cases, when system response is excited by a steplike wind gust of assigned magnitude.

This Note is organized as follows. In Sec. II, the reference LV model, representative of a medium-size vehicle (liftoff mass of 120,000 kg) of the same payload class as VEGA, is presented. In Sec. III, the main elements of a FCS featuring a BC with adaptive augmentation are recalled. Section IV illustrates the AAC tuning techniques, and Sec. V presents the main results on the optimally tuned AAC performance. A section of Conclusions ends the Note.

II. Vehicle Model

A linear time-varying model, the detailed description of which can be found in Refs. [8,10], is considered for LV analysis in atmospheric flight. It accounts for rigid-body pitch-axis rotational and lateral drift dynamics with respect to vehicle reference trajectory, together with contributions of first bending mode and nozzle actuation dynamics, whereas aerodynamic damping and tail-wags-dog (TWD) effects are neglected. The latter assumptions are coherent with the level of accuracy of the model and somewhat conservative because TWD effects, which usually occur at a frequency between the first and second bending modes, would be slightly stabilizing for the present LV configuration. Also, aerodynamic damping terms would influence the stability of elastic mode higher than first, whereas the effects on the rigid modes of the controlled LV are negligible [11]. The model represents a symmetric LV configuration where, for the purpose of attitude control system design, the couplings between pitch and yaw dynamics are ruled out, and the single rotational degree of freedom may be associated to either pitch or yaw motion.

The governing equations are written as

$$\begin{bmatrix} \dot{z} \\ \ddot{z} \\ \dot{\theta} \\ \ddot{\theta} \\ \dot{q} \\ \ddot{q} \end{bmatrix} = \begin{bmatrix} 0 & 1 & 0 & 0 & 0 & 0 \\ 0 & -\dfrac{N_\alpha}{mV} & \dfrac{D-T_t-N_\alpha}{m} & 0 & 0 & 0 \\ 0 & 0 & 0 & 1 & 0 & 0 \\ 0 & \dfrac{N_\alpha l_\alpha}{I_{yy}}/V & \dfrac{N_\alpha l_\alpha}{I_{yy}} & 0 & 0 & 0 \\ 0 & 0 & 0 & 0 & 0 & 1 \\ 0 & 0 & 0 & 0 & -\omega_{\mathrm{BM}}^2 & -2\zeta_{\mathrm{BM}}\omega_{\mathrm{BM}} \end{bmatrix} \begin{bmatrix} z \\ \dot{z} \\ \theta \\ \dot{\theta} \\ q \\ \dot{q} \end{bmatrix} + \begin{bmatrix} 0 \\ \dfrac{T_c}{m} \\ 0 \\ \dfrac{T_c l_c}{I_{yy}} \\ 0 \\ -\hat{\phi}_{\mathrm{TVC}} T_c \end{bmatrix} \beta + \begin{bmatrix} 0 \\ \dfrac{N_\alpha}{m} \\ 0 \\ -\dfrac{N_\alpha l_\alpha}{I_{yy}} \\ 0 \\ 0 \end{bmatrix} \alpha_w \tag{1}$$

where z and $\dot{z}$ are, respectively, the drift and drift rate of the center of mass along the normal axis of the trajectory frame, θ is the perturbed pitch angle, q is the generalized coordinate of the first elastic mode, β is the nozzle angle, and $\alpha_w = v_w/V$ is the wind-induced angle of attack, with V and v_w as the flight speed and wind velocity, respectively. Also, m and I_{yy} are the LV mass and moment of inertia, l_α and l_c are the aerodynamic and control moment arms, $T_t = T_s + T_c$ is the total thrust force made of sustained thrust T_s and control (swiveled) thrust T_c, N_α is the aerodynamic normal force acting on the center of pressure, and D is the aerodynamic axial force. Finally, ω_{BM}, ζ_{BM}, and $\hat{\phi}_{\mathrm{TVC}}$ are, respectively, the bending mode natural frequency, damping ratio, and displacement component over generalized mass at the thrust vector control (TVC) location.

[¶]A min-max problem seeks to minimize the maximum value of a number of decision variables.

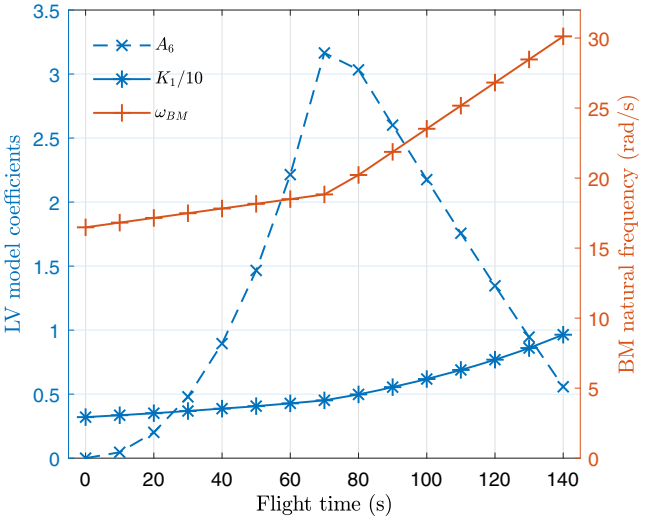

Fig. 1 Aerodynamic and control moment coefficients, and bending mode natural frequency vs flight time.

According to typical notation for LV dynamic models [12], the following parameters are defined:

$$A_6 = \frac{N_\alpha l_\alpha}{I_{yy}} \quad K_1 = \frac{T_c l_c}{I_{yy}} \quad a_1 = -\frac{N_\alpha}{mV} \quad a_3 = \frac{T_c}{m} \quad a_4 = -\frac{(T_t - D)}{m}$$

where A_6 and K_1 are dubbed, respectively, aerodynamic and control moment coefficients.

The output vector $y = [\,\theta_{\mathrm{INS}} \quad \dot{\theta}_{\mathrm{INS}} \quad z_{\mathrm{INS}} \quad \dot{z}_{\mathrm{INS}}\,]^T$ is expressed as

$$y = \begin{bmatrix} 0 & 0 & 1 & 0 & \sigma_{\mathrm{INS}} & 0 \\ 0 & 0 & 0 & 1 & 0 & \sigma_{\mathrm{INS}} \\ 1 & 0 & 0 & 0 & -\phi_{\mathrm{INS}} & 0 \\ 0 & 1 & 0 & 0 & 0 & -\phi_{\mathrm{INS}} \end{bmatrix} \begin{bmatrix} z \\ \dot{z} \\ \theta \\ \dot{\theta} \\ q \\ \dot{q} \end{bmatrix} \tag{2}$$

where ϕ_{INS} and σ_{INS} represent, respectively, bending mode displacement and rotation components at the location of inertial navigation system.

Nozzle angle β generated by thrust vector control depends on actuator dynamics and a pure delay τ that accounts for hardware processing time. In particular, using a second-order Padé approximation and, being β_c the TVC command, gives

$$\begin{bmatrix} \dot{d} \\ \ddot{d} \end{bmatrix} = \begin{bmatrix} 0 & 1 \\ -\dfrac{12}{\tau^2} & -\dfrac{6}{\tau} \end{bmatrix} \begin{bmatrix} d \\ \dot{d} \end{bmatrix} + \begin{bmatrix} 0 \\ -\dfrac{12}{\tau} \end{bmatrix} \beta_c \tag{3}$$

and $\beta_{\hat{c}} = \dot{d} + \beta_c$. The actuator transfer function is

$$W_{\mathrm{TVC}}(s) = \frac{\beta}{\beta_{\hat{c}}} = \frac{\omega_{\mathrm{TVC}}^2}{s^2 + 2\zeta_{\mathrm{TVC}}\omega_{\mathrm{TVC}} s + \omega_{\mathrm{TVC}}^2} \tag{4}$$

where ζ_{TVC} and ω_{TVC} are the damping ratio and natural frequency, respectively.

Variations of principal LV parameters (that is, A_6, K_1, and ω_{BM}) as functions of flight time are shown in Fig. 1 for a representative ascent trajectory from launch pod through an altitude of 60 km. The model data at the maximum dynamic pressure (max-$\bar{q}$) condition ($t = 72$ s) are reported in Table 1. The LV dataset[**] is retrieved from appendix A

[**]The LV model is freely available on GitHub at https://github.com/AlessandroZavoli/Rocket-Attitude-Dynamics for FCS performance evaluation and benchmarking.

Table 1 LV model parameters at $t = 72$ s (max-$\bar{q}$ condition)

	Unit	Value
m	kg	7.38×10^4
l_α	m	10.39
l_c	m	9.84
I_{yy}	kg · m^2	3.28×10^6
V	m/s	937.70
Alt	m	15, 143
T_c	N	1.52×10^6
$T_t - D$	N	1.71×10^6
N_α	N/rad	1.07×10^6
A_6	1/s^2	3.3818
K_1	1/s^2	4.5647
a_1	1/s^2	−0.0154
a_3	1/s^2	20.6090
a_4	1/s^2	−27.2710
ω_{BM}	rad/s	18.9
ζ_{BM}	— —	0.005
ϕ_{INS}	— —	0.8
σ_{INS}	rad/m	0.178
$\hat{\phi}_{\mathrm{TVC}}$	1/kg	4.31×10^{-5}
ω_{TVC}	rad/s	70
ζ_{TVC}	— —	0.7

of Ref. [11] and chapter 3 of Ref. [13]. A number of simulations were run to validate the model, checking consistency with expected behavior and coherency, including the effects of parameter variations on stability, with available models of LVs of the same class such as the VEGA launcher.

The considered profile of wind velocity v_w represents a step gust that slowly decays over time so as to excite the system dynamics around the max-$\bar{q}$ condition in a wide frequency range for the goal of AAC tuning. It is given by

$$v_w(t) = \begin{cases} V_a \left(\dfrac{t}{t_a}\right)^2 & \text{for } 0 \le t < t_a \\ (V_b - V_a)\dfrac{t - t_a}{t_b - t_a} + V_a & \text{for } t_a \le t \le t_b \\ V_b e^{(t-t_b/t_f-t_b)\log(0.1/V_b)} & \text{for } t_b < t \le t_f \end{cases} \tag{5}$$

where the coefficients are specified as $t_f = 100$ s, $t_a = 70$ s, $t_b = 75$ s, $V_a = 5$ m · s^{-1}, and $V_b = -30$ m · s^{-1}.

III. Flight Control System

Typical architecture of a LV control system with the AAC generating a multiplicative gain for BC output is sketched in Fig. 2. Details on the elements of the adaptive controller are reported in Ref. [2]. Major FCS design requirements, to be satisfied in nominal and dispersed flight conditions, are 1) to stabilize LV attitude, 2) to maintain the vehicle on the programmed trajectory, 3) to limit the aerodynamic loads while rejecting external disturbances, and 4) to use minimal adaption in nominal conditions when control is entirely managed by the BC. In what follows, the BC design is discussed first, according to traditional and well-established criteria in LV control; next, the guidelines adopted so far for AAC tuning are recalled.

A. Baseline Controller

The BC features two proportional–derivative (PD) components for attitude and translational motion control, plus filters to phase stabilize and notch the bending modes [11,12]. The controller, fed by the output vector $\boldsymbol{y}$, is

$$\boldsymbol{K}_{\mathrm{BC}}(s) = [\,K_{P_\theta} \quad K_{D_{\dot\theta}} \quad K_{P_z} \quad K_{D_{\dot z}}\,] H_X(s) H_N(s) \tag{6}$$

where K_{P_θ}, $K_{D_{\dot\theta}}$, K_{P_z}, and $K_{D_{\dot z}}$ are, respectively, the gains on pitch and z-axis channels; H_X is a second-order nonminimum phase low-pass filter; and H_N is a notch filter.

Pitch-axis control gains are obtained by enforcing classic stability requirements to the reduced system obtained neglecting lateral dynamics, TVC, and bending mode dynamics [12]: that is, a 6 dB gain margin at low frequency and a 30 deg phase margin at high frequency so as to obtain [14]

$$K_{P_\theta} = \frac{2A_6}{K_1} \qquad K_{D_{\dot\theta}} = \frac{\sqrt{A_6}}{K_1} \tag{7}$$

Gains for lateral control are to be small in order to guarantee system stability while limiting maximum drift-rate and z-axis displacement. Therefore, the values of K_{P_z} and K_{D_z} at max-$\bar{q}$ are specified, respectively, as 1×10^{-3} rad/m and 4.5×10^{-5} rad/(m/s) in order to obtain maximum values of $\dot z$ and z of the order of 10 m/s and 300 m, respectively, without hindering the controller performance on attitude error.

As reported in Ref. [15], the notch filter is realized by three cascaded second-order filters centered, respectively, at the nominal bending mode frequency ω_{BM} and $\omega_{\mathrm{BM}} \pm 10\%$. The overall transfer function is

$$H_N(s) = \frac{s^2 + 2\zeta_N \underline{\omega}_{\mathrm{BM}} s + \underline{\omega}_{\mathrm{BM}}^2}{s^2 + 2\zeta_D \underline{\omega}_{\mathrm{BM}} s + \underline{\omega}_{\mathrm{BM}}^2} \cdot \frac{s^2 + 2\zeta_N \omega_{\mathrm{BM}} s + \omega_{\mathrm{BM}}^2}{s^2 + 2\zeta_D \omega_{\mathrm{BM}} s + \omega_{\mathrm{BM}}^2} \cdot \frac{s^2 + 2\zeta_N \overline{\omega}_{\mathrm{BM}} s + \overline{\omega}_{\mathrm{BM}}^2}{s^2 + 2\zeta_D \overline{\omega}_{\mathrm{BM}} s + \overline{\omega}_{\mathrm{BM}}^2} \tag{8}$$

where $\underline{\omega}_{\mathrm{BM}} = 0.9\omega_{\mathrm{BM}}$ and $\overline{\omega}_{\mathrm{BM}} = 1.1\omega_{\mathrm{BM}}$. The values of parameters ζ_N and ζ_D, with $\zeta_N < \zeta_D$, that specify the bandwidth and peak level of filter attenuation, respectively, are $\zeta_N = 0.02$ and $\zeta_D = 0.1$.

Phase stabilization is realized when the phase of elastic dynamics is near 0 deg (in general, between −180 and 180 deg). To this end a nonminimum phase, second-order low-pass filter

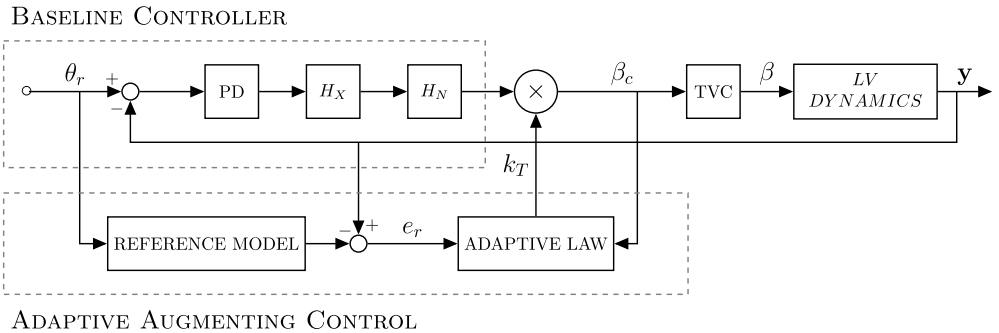

Fig. 2 Architecture of LV control system with AAC.

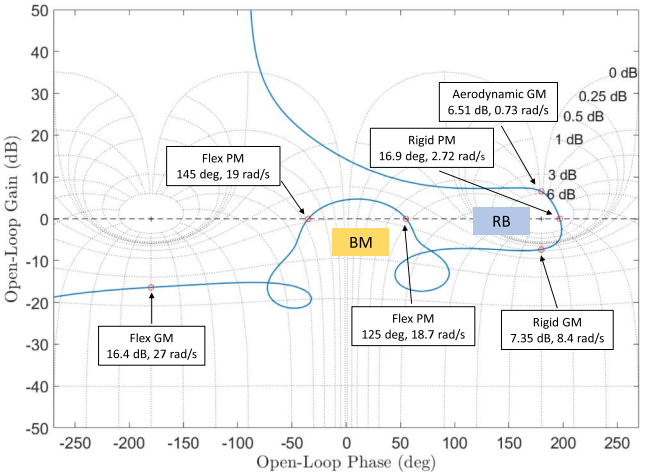

Fig. 3 Nichols chart of LV model open-loop response at $t = 72$ s.

$$H_X(s) = \frac{s^2 + 2\zeta_z\omega_z s + \omega_z^2}{s^2 + 2\zeta_p\omega_p s + \omega_p^2} \tag{9}$$

is considered [16]. Pole and zero locations are specified so that they share the same natural frequency (close to ω_{BM}) with $\zeta_p > \zeta_z$, and the values $\zeta_p = 0.5$ and $\zeta_z = 0.2$ have been selected. Gains and filter parameters are scheduled versus time over a 10 s time grid, and they are linearly interpolated throughout the flight.

A Nichols plot of the open-loop response for the LV model at $t = 72$ s is shown in Fig. 3. The frequency response presents two groups of stability margins. The first one includes low-frequency margins (frequency below 8.4 rad/s) [namely, aerodynamic gain margin (GM), rigid GM, and rigid phase margin (PM)] that are associated to the rigid-body (RB) dynamics. The group of high-frequency margins (frequency above 8.4 rad/s; that is, flex GM and flex PM) refer to the bending mode (BM). The hump of the curve between the critical points confirms the bending mode attenuation and phase stabilization realized by the filters.

B. Adaptive Augmenting Control Design

Adaptive control [2] regulates the BC output by means of a multiplicative gain $k_T = k_0 + k_a$, where $k_0 > 0$ is a design parameter and $k_a > 0$ is given by

$$\dot{k}_a = \left(\frac{k_{\max} - k_a}{k_{\max}}\right) a_{\mathrm{AAC}} e_r^2 - \alpha_{\mathrm{AAC}} k_a y_s - \beta_{\mathrm{AAC}}(k_T - 1) \tag{10}$$

The first term in Eq. (10), called the model-reference error, increases the gain proportionally to the squared error of a reference model that approximates the closed-loop dynamics of the vehicle [4], expressed as $e_r = \theta_{\mathrm{INS}} - \theta_r$. Since the reference frame is tangent to the nominal trajectory, the preceding angle θ_{INS} represents the angular displacement relative to the nominal condition, and θ_r is zero for the entire flight.

The limit $(k_{a_{\max}} - k_a)/k_{a_{\max}}$ prevents divergence of adaptive gain because $k_{a_{\max}}$ is to be equal to the gain margin in nominal conditions in order to avoid instability.

The *spectral damper* term reacts to undesired high-frequency dynamics in the control signal by reducing the adaptive gain. The input y_s is computed as

$$y_s = H_{\mathrm{LP}}(s) y_{\mathrm{HP}}^2 \tag{11}$$

$$y_{\mathrm{HP}} = H_{\mathrm{HP}}(s)\beta_c \tag{12}$$

where H_{LP} and H_{HP} are, respectively, second-order filters that identify the high-frequency content of β_c and quantify the average spectral power of the input given by

$$H_{\mathrm{HP}} = \frac{s^2 + 2\omega_z^{\mathrm{HP}} s + \omega_z^{\mathrm{HP}^2}}{s^2 + 2\omega_p^{\mathrm{HP}} s + \omega_p^{\mathrm{HP}^2}} \quad H_{\mathrm{LP}} = K\frac{s^2 + 2\omega_z^{\mathrm{LP}} s + \omega_z^{\mathrm{LP}^2}}{s^2 + 2\omega_p^{\mathrm{LP}} s + \omega_p^{\mathrm{LP}^2}} \tag{13}$$

where $K = 0.0032$, and the other parameters are expressed in terms of the cutoff frequencies ω_c^{HP} and ω_c^{LP} as [7,8]

$$\omega_p^{\mathrm{HP}} = 0.7\omega_c^{\mathrm{HP}} \quad \omega_z^{\mathrm{HP}} = 10^{-5/4}\omega_p^{\mathrm{HP}} \quad \omega_p^{\mathrm{LP}} = 1.6\omega_c^{\mathrm{LP}} \quad \omega_z^{\mathrm{LP}} = 10^{5/4}\omega_p^{\mathrm{LP}}$$

Finally, the *leakage* term in Eq. (10) forces k_T to unity because, as said, LV control is expected to be fully on charge of BC in nominal conditions.

The current approach for tuning an The current approach for AAC tuning consists of setting three main elements [2]: 1) upper and lower bounds of the adaptive gain k_T equal, respectively, to the low- and high-frequency gain margins (namely, $\mathrm{GM}_{\mathrm{aero}}$ and $\mathrm{GM}_{\mathrm{rigid}}$) related to the rigid-body dynamics of the nominal system; 2) cutoff frequency of the spectral damper filters, ω_c^{HP} and ω_c^{LP}; and 3) gains a_{AAC}, α_{AAC}, and β_{AAC}. The latter two sets of parameters are specified by relying on time-consuming trial-and-error procedures [2,7].

As a final comment on AAC, an evolved formulation of the adaptive gain law is discussed in Ref. [4], which is written as

$$\dot{k}_T = p_{\mathrm{hi}}(k_T) a_{\mathrm{AAC}} e_r^2 - p_{\mathrm{lo}}(k_T)\alpha_{\mathrm{AAC}} y_s - \beta_{\mathrm{AAC}}(k_T - 1) \tag{14}$$

where p_{hi} and p_{lo} are saturation functions that do not require specific tuning. It is apparent the two AAC algorithms [Eqs. (10) and (14)] share the same structure so that the proposed approach to optimal tuning, devised for the basic form of the adaptive law, can be also applied to its modified version.

IV. Optimal AAC Tuning

The tuning methodologies are based on the metrics $J_1 = \|\Delta\theta\|_\infty$ and $J_2 = \|H_{\mathrm{HP}}\Delta\theta\|_1$ that measure FCS performance in a (single) time-domain simulation with respect to maximum angular displacement and unwanted oscillatory behavior, respectively, over the considered flight phase.

A. RDO/MC Approach

In the first approach, a problem dubbed RDO/MC is formulated as follows. Let c be a randomly generated realization of a scattered subset of LV coefficients, according to a prescribed uncertainty distribution. The vector $\boldsymbol{x} = [a_{\mathrm{AAC}}, \alpha_{\mathrm{AAC}}, \beta_{\mathrm{AAC}}, \omega_c^{\mathrm{HP}}, \omega_c^{\mathrm{LP}}]^T$ of tuning parameters is determined that minimizes a combined merit index J_{MC} based on the worst performance, in terms of J_1 and J_2, across a set $\mathcal{C}$ of realizations $c \in \mathcal{C}$ that, in fact, is a Monte Carlo simulation campaign. The optimization problem is written as

$$\min_x J_{\mathrm{MC}}(\boldsymbol{x}) = \min_x \left\{ \max_{c\in\mathcal{C}} J_1^{(c)} + \max_{c\in\mathcal{C}} J_2^{(c)} \right\} \tag{15}$$

where, following a few tests, it turns out that $\|\mathcal{C}\| = 100$ can provide a consistent statistic evaluation of J_{MC}.

A genetic algorithm (GA) [17] is used for solving the RDO/MC problem. GAs are well-known population-based derivative-free metaheuristic techniques inspired by natural evolution that have been successfully applied to a wide range of real-world problems of significant complexity. The GA performs a global optimization and, thanks to its stochastic selection and mutation operators, has greater chances to evade local optima than greedy methods. Although population-based methods usually result in an order of magnitude lower convergence rate than deterministic optimization algorithms, adoption of the GA for problem (15) is motivated by the fact that the objective function J_{MC} is nondifferentiable and intrinsically noisy because it is the result of a number of Monte Carlo simulations. In this respect, the GA peculiarity of replacing most (if not all) of the population at each generation dramatically improves the success over other metaheuristic algorithms [17]. To enhance the GA convergence properties, an appropriate combination of the fundamental genetic operators is adopted, that is, K-random tourney selection, simulated

binary crossover with probability $p_c = 0.9$, and adaptive uniform mutation with probability $p_m = 0.05$. Algorithm performance is further improved by using elitism to ensure monotonic improvement in the best solution at any generation, as well as a partial restart mechanism that activates whenever the population diversity is low, in order to avoid premature stagnation of the population to a suboptimal solution. Further details on the GA optimization can be found in Ref. [18].

B. RDO/Min-Max Approach

The second tuning method should address the major issues experienced in the application of RDO/MC (that is, high computational cost and noisy objective function J_{MC} due to the quality of the approximate randomness generated by MC simulations), exploiting actual practices in AAC application to LV attitude control systems. According to prior investigations [8], a suitable tuning of spectral damper can be achieved by selecting the cutoff frequencies as functions of the rigid-body GM frequency $\omega_{\mathrm{GM\,rigid}}$: that is, $\omega_c^{\mathrm{HP}} = \omega_{\mathrm{GM\,rigid}}$ and $\omega_c^{\mathrm{LP}} = \omega_c^{\mathrm{HP}}/2$. The other gains a_{AAC}, α_{AAC}, and β_{AAC} define the relative weight of the model-reference error, spectral damper, and leakage terms, respectively. Since the leakage is usually well behaved, provided that a sufficiently small value of β_{AAC} is selected in the range $[0.05, 0.3]$, $\beta_{\mathrm{AAC}} = 0.25$ is hereafter assumed.

In facts, the design problem consists of tuning the remaining parameters $\tilde{\boldsymbol{x}} = [\alpha_{\mathrm{AAC}}, a_{\mathrm{AAC}}]$ and, to this end, Ref. [8] shows that two limiting cases, due to parameter variations or off-nominal operations, may cause high values of either the reference model error or the spectral damper output. More precisely, when the system operates with a nearly zero low-frequency rigid-body GM (aerodynamic GM), the large reference model error (and related term) provides the increment of total adaptive gain k_T necessary to recover the stability margin. Conversely, whenever the high-frequency rigid-body GM (rigid GM) gets close to zero, k_T is reduced by the spectral damper action to, again, preserve system stability.

Therefore, a set of realizations $\mathcal{C}^\star = \{c_{A-\mathrm{GM}}, c_{R-\mathrm{GM}}\}$ is specified with reference to the aforementioned situations; that is, $c_{A-\mathrm{GM}}$ is defined by increasing A_6 and decreasing K_1 by the same amount until the aerodynamic GM approximates zero, whereas $c_{R-\mathrm{GM}}$ is obtained by reducing the elastic mode frequency ω_{BM} until the rigid GM becomes negligible while keeping A_6 and K_1 at their nominal values. The design goal is thus to optimize FCS performance with respect to the most demanding (in term of control action) of the two limit conditions, once a steplike wind gust [Eq. (5)] is assigned as disturbance. As a result, the RDO/min-max optimization problem is formulated as

$$\min_{\tilde{x}} J(\tilde{\boldsymbol{x}}) = \min_{\tilde{x}} \left\{ \max_{c\in\mathcal{C}^\star} J_1^{(c)} + \max_{c\in\mathcal{C}^\star} J_2^{(c)} \right\} \tag{16}$$

that can be regarded as a scaled-down form of problem (15), where only two simulations per objective function evaluation are needed and, as an advantage, the objective function J is well behaved with respect to the MC-based function J_{MC}.

The RDO/min-max problem is tackled by the Nelder–Mead simplex method [19] (a local derivative-free optimization technique) so as improve convergence by limiting numerical errors in the finite difference evaluation of J derivatives. Provided that a reasonable initial guess is given, convergence is about one order of magnitude faster than a population-based global optimization algorithm. Global optimality of the solution can be pursued by repeatedly performing a random-start (or multiple-start) initialization procedure.

It is worth mentioning that, although (as said) a deterministic wind disturbance is applied to each simulation run, the technique could be easily extended to incorporate other limiting conditions that may be pertinent to a specific LV and/or accommodate realistic wind profiles if appropriate: for instance, introducing real in-flight wind measurements from previous missions.

V. Discussion

Table 2 shows the AAC tuning parameters evaluated according to the two procedures. As for the bounds on k_T, the values $k_0 = \mathrm{GM}_{\mathrm{aero}}$ and $k_{a_{\max}} = \mathrm{GM}_{\mathrm{rigid}} - k_0$ are set, where the small margins in the max-$\bar{q}$ condition (critical for stability) are taken into consideration. It is apparent that the optimal solutions present minor differences, as expected to some extent. The point is that the RDO/min-max method is significantly more efficient from a computational point of view. In particular, the solution is determined in about 15 min using an Intel Core i7-9700K CPU at 3.60 GHz with eight physical cores in spite of the fact that Nelder–Mead is a serial algorithm, whereas the RDO/MC approach takes roughly 16 h on the same hardware while running a fully parallel algorithm. In this respect, it is worth remarking that the deterministic Nelder–Mead simplex method can be effectively used for the RDO/min-max optimization in place of the stochastic GA because of the minor complexity of the problem and the smoother cost function.

As for RDO/MC, a minor tweaking of GA hyperparameters is required in order to improve convergence and, notably, suitable values of the population size N_P and number of generations N_G are to be selected. After a few tests showing that large values of the aforementioned parameters significantly increase computational time without improving quality of solution, N_P and N_G were set to 64 and 100, respectively.

Performance assessment for the FCS is carried out through extensive sets of simulations in the time domain that consider the LV flight from liftoff to the first stage separation for a wide scattering range of model parameters, as shown in Table 3. Stochastic disturbances are generated by a Dryden wind model, specialized according to NASA guidelines [20] as recalled in Ref. [21]; conditions of severe turbulence are considered in all simulations.

Tuning approaches are robust against the wind profiles used in the optimization process. This is demonstrated in Fig. 4, where the envelopes of the structural load $\bar{q}\alpha$ computed from MC campaigns of 1000 simulations are shown for the FCS using the AAC tuned with two different wind profiles: that is, the step gust in Eq. (5) and a randomly generated wind based on the Dryden model [20] (Fig. 4a). It is apparent in Fig. 4b that the wind profile used for tuning (the RDO/min-max method is adopted) has no effect on AAC performance because the two envelopes are indistinguishable. Similar results are obtained with different wind profiles, provided that a smooth and reasonably large variation of v_w near the max-$\bar{q}$ condition is specified.

Figure 5 shows the L_2 norm of the attitude error $\Delta\theta$, drift z and drift rate $\dot{z}$, and structural load $\bar{q}\alpha$ together with the overall control effort (i.e., $\|\beta\|_1$) as computed for the AAC using the two tuning solutions. The norms are averaged over 1000 simulations (model

Table 2 AAC optimally tuned parameters

Tuning method	k_0	$k_{a_{\max}}$	a_{AAC}	α_{AAC}	β_{AAC}	ω_c^{HP}	ω_c^{LP}
RDO/min-max	0.50	1.50	3,192.00	22,806.00	0.25	8.00	4.00
RDO/MC	0.50	1.50	3,856.00	43,277.00	0.17	8.77	1.67

Table 3 Scattering ranges for Monte Carlo simulations

Parameter	Scattering range, %
A_6	±30
K_1	±30
a_1	±10
a_3	±10
a_4	±10
ω_{BM}	±30

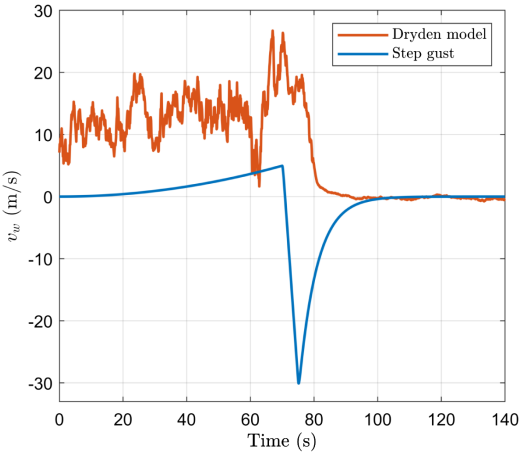

a) Wind profiles for AAC tuning

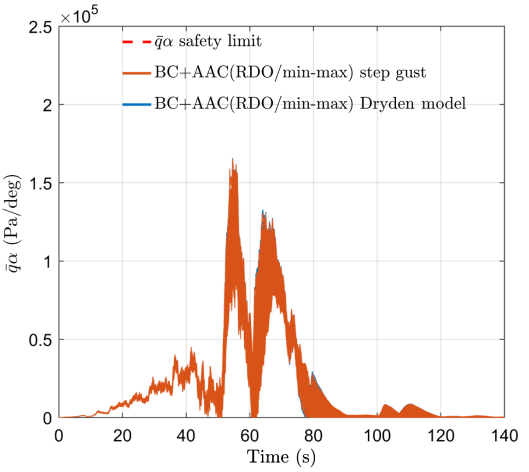

b) $\bar{q}\,\alpha$ envelope and safety limit vs time: model parameters scattered as in Table 3, single wind profile

Fig. 4 Effect of wind profile on AAC tuning.

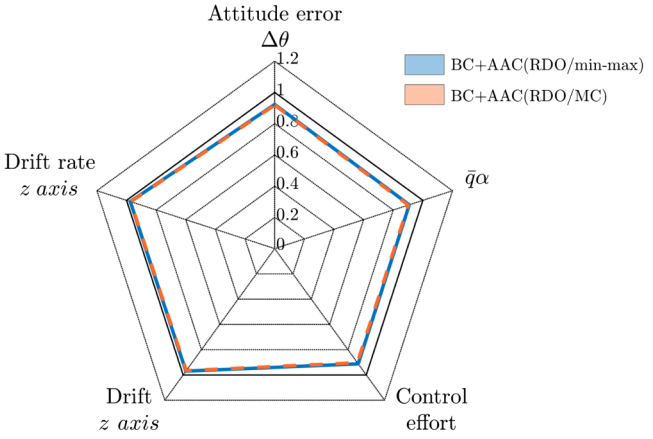

Fig. 5 Normalized performance metrics over a Monte Carlo campaign based on 1000 simulations.

parameters are scattered according to Table 3) and normalized with respect to the same metrics computed for the LV controlled by the BC without augmentation. The results for the two formulations of the minimization problem are, in fact, indistinguishable, as was expected given the close values of optimal AAC gains. Control system performance is improved by AAC in terms of $\bar{q}\alpha$ (-13%) and attitude error (-8%) while keeping the same performance levels as BCs on z-axis drift rate and displacement.

Further insight in the outcome of AAC optimal tuning is provided in Table 4, where the effects of the adaptive law are shown in terms of L_∞ norms of $\Delta\theta$, z, $\dot{z}$, and $\bar{q}\alpha$, which are averaged over the MC runs. It is apparent that, even in terms of worst performance, $\bar{q}\alpha$ and the attitude error are reduced, whereas $\dot{z}$ and (to an even lesser extent) z are only slightly affected by the adaptive law. The latter is due to the fact that the adaptive gain k_T depends on z-drift only indirectly, through the system dynamics.

Table 4 Average L_∞ norm of performance parameters from Monte Carlo simulations

Controller	$\|\Delta\theta\|_\infty$, deg	$\|z\|_\infty$, m	$\|\dot{z}\|_\infty$, m/s	$\|Q\alpha\|_\infty$, kPa/ deg
BC	4.45	136.33	13.26	13.41
BC + AAC (RDO/MC)	4.04	136.13	12.58	11.73
BC + AAC (RDO/min-max)	4.05	136.48	12.62	11.79

It is worth observing that AAC performance assessment by averaging the aforementioned metrics over a large number of cases (many of which are easily managed by the BC) does not properly represent the results and benefits of AAC action. In this respect, Fig. 6 shows the envelope of $\bar{q}\alpha$ together with the corresponding safety limit [10] over a Monte Carlo campaign based on 1000 simulation runs, where model parameters are scattered as in Table 3 and a single wind profile is considered in all runs. Controller performances are compared for the LV featuring BC (Fig. 6a) and the BC with augmentation: that is, RDO/min-max and RDO/MC tunings in Figs. 6b and 6c, respectively. It is apparent in the figures, where the time histories of $\bar{q}\alpha$ for nominal values of the parameters are also reported as bold continuous lines, that the two methodologies for optimal tuning provide similar results. Considering that simulations where $\bar{q}\alpha$ exceeds the threshold may end up with a LOV event (that is, a mission failure), the benefit of the AAC on mission success rate is now clearly visible because RDO/min-max tuning prevents 270 out of 295 situations where the safety limit is violated that would have occurred without augmentation. Note that such a large number of cases with $\bar{q}\alpha$ above threshold is due to the combined effects of an extended scattering range and a tight safety envelope.

As said, adaptive algorithms developed for the SLS have evolved and been consolidated over time. In this respect, the suitability of the proposed tuning approaches for the AAC formulation [4] is investigated through the application of the RDO/min-max approach to determine the gains a_{ACC} and α_{ACC} in Eq. (14). Figure 7 shows the structural load vs time for the same MC campaign reported in Fig. 6 (parameter scattering of Table 3 and single wind profile). The FCS performance obtained with the advanced law [Eq. (14)] is comparable to that provided by the algorithm [Eq. (10)] considered in this study.

A closer and final view of simulation outcome shows that AAC can successfully deal with scattering of rigid-body parameters as large as 30%, whereas relevant variations of bending mode frequency are more troublesome (mostly when the frequency decreases), particularly when the spectral damper is not properly tuned. In those circumstances, the AAC may occasionally degrade BC performance, and even lead the system to instability, as gain stabilization can hardly manage large offsets from nominal of elastic mode characteristics.

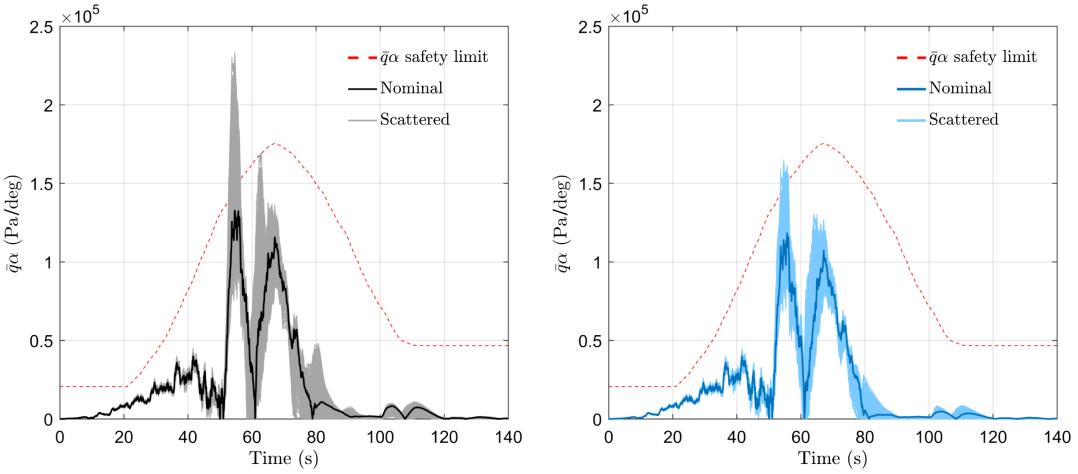

a) BC b) BC + AAC (RDO/min-max)

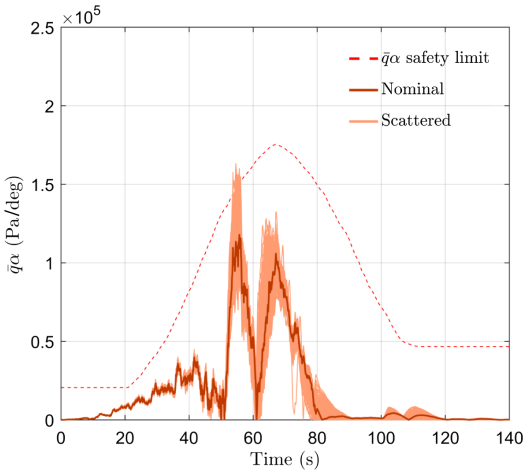

c) BC + AAC (RDO/MC)

Fig. 6 $\bar{q}\alpha$ envelope and safety limit vs time: model parameters scattered as in Table 3, single wind profile; bold continuous lines indicate no scattering.

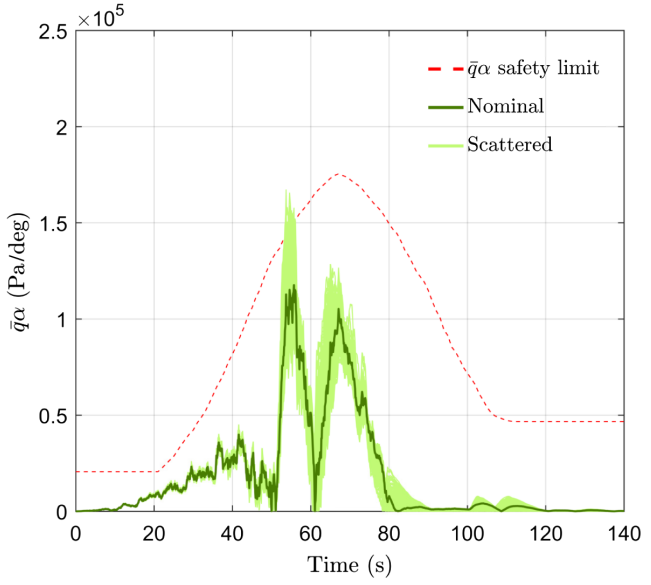

Fig. 7 Application of RDO/min-max tuning procedure to evolved AAC [Eq. (14)]: $\bar{q}\alpha$ envelope and safety limit vs time; model parameters scattered as in Table 3, single wind profile; bold continuous line indicates no scattering.

VI. Conclusions

In this Note, two novel and effective tuning methodologies for an adaptive augmenting control system, realized to consistently improve performance and robustness of a standard launch vehicle single–axis attitude controller in atmospheric flight, have been presented. As a major advantage, the issues and burden of the manual trial-and-error procedures currently adopted for the design of the adaption law can be reduced.

The first approach, which involves the solution of a robust design optimization (RDO) problem where the objective function (J_{MC}) evaluation requires the computational effort of a Monte Carlo (MC) campaign, prevents convergence to local minima, and is robust with respect to initial estimates of tuning parameters and unsmooth J_{MC}. The optimization problem can be implemented with minor difficulties using a standard genetic solver. On the other hand, the RDO/min-max method provides the same quality of results, being much faster and less computationally demanding, because the performance metrics are determined in a few suitably selected, corner cases. The tuning procedures provide similar adaptive laws that improve the BC performance in terms of attitude error and angle-of-attack limitation, preventing up to 94% of events that could determine a loss-of-vehicle situation in the current tests. To augment robustness to variations of elastic mode parameters, the AAC architecture should probably be integrated with adaptive notch-filters to provide phase-stabilization for at least the first bending mode.

As a final comment, AAC can be an effective and reliable tool for enhancing flight control system robustness with respect to parametric uncertainties and, possibly, a mean for limiting the costs of

mission integration activities; in this respect, adoption of a systematic tuning methodology might positively impact on time and workload dedicated to flight program software finalization for different LV missions.

Acknowledgment

This work was supported by European Space Agency's European Space Research Institute (ESA-ESRIN) under grant no. 4000120618/17/I/AL.

References

[1] Creech, S., May, T., and Robinson, K., "NASA's Space Launch System: An Enabling Capability for International Exploration," *IAA Space Exploration Conference, M14-3167*, International Academy of Astronautics Paper WAS0517, 2014.

[2] Orr, J., and Van Zwieten, T., "Robust, Practical Adaptive Control for Launch Vehicles," *AIAA Guidance, Navigation, and Control Conference*, AIAA Paper 2012-4549, 2012. https://doi.org/10.2514/6.2012-4549

[3] Orr, J., Wall, J., VanZwieten, T., and Hall, C., "Space Launch System Ascent Flight Control Design," *Advances in the Astronautical Sciences*, Vol. 151, 2014, pp. 141–154; also American Astronomical Soc. Paper 14-038, San Diego, CA, 2014.

[4] Wall, J. H., Orr, J. S., and VanZwieten, T. S., "Space Launch System Implementation of Adaptive Augmenting Control," *37th Annual American Astronautical Society (AAS) Guidance, Navigation, and Control Conference*, American Astronomical Soc. Paper 14-051, San Diego, CA, 2014.

[5] Clements, K., and Wall, J., "Time Domain Stability Margin Assessment of the NASA Space Launch System GN&C Design for Exploration Mission One," *AAS Guidance and Control Conference*, American Astronomical Soc. Paper 17-126, San Diego, CA, 2017.

[6] VanZwieten, T. S., Hannan, M. R., and Wall, J. H., "Evaluating the Stability of NASA's Space Launch System with Adaptive Augmenting Control," *CEAS Space Journal*, Vol. 10, No. 4, 2018, pp. 583–595. https://doi.org/10.1007/s12567-018-0211-y

[7] Navarro-Tapia, D., Marcos, A., Bennani, S., and Roux, C., "Robust-Control-Based Design and Comparison of an Adaptive Controller for the VEGA Launcher," *AIAA SciTech 2019 Forum*, AIAA Paper 2019-0649, 2019. https://doi.org/10.2514/6.2019-0649

[8] Trotta, D., Zavoli, A., De Matteis, G., and Neri, A., "Opportunities and Limitations of Adaptive Augmented Control for Launch Vehicle Attitude Control in Atmospheric Flight," *Astrodynamics Specialist Conference*, American Astronautical Soc. Paper 19-765, San Diego, CA, 2019.

[9] Beyer, H.-G., and Sendhoff, B., "Robust Optimization—A Comprehensive Survey," *Computer Methods in Applied Mechanics and Engineering*, Vol. 196, Nos. 33–34, 2007, pp. 3190–3218. https://doi.org/10.1016/j.cma.2007.03.003

[10] Greensite, A. L., "Analysis and Design of Space Vehicle Flight Control Systems. Volume I-Short Period Dynamics," NASA CR-820, GD/C-DDE65-055, 1967.

[11] Greensite, A. L., "Analysis and Design of Space Vehicle Flight Control Systems. Volume VII-Attitude Control During Launch," NASA CR-826, GD/C-DDE66-028, 1967.

[12] Roux, C., and Cruciani, I., "Scheduling Schemes and Control Law Robustness in Atmospheric Flight of VEGA Launcher," *Proceedings of the 7th ESA International Conference on Spacecraft Guidance, Navigation and Control Systems*, June 2008, pp. 1–5.

[13] Greensite, A. L., "Analysis and Design of Space Vehicle Flight Control Systems. Volume II-Trajectory Equations," NASA CR-821, GD/C-DDE65-058, 1967.

[14] Gadea Daz, E., "Design of a Robust Controller for the VEGA TVC Using the μ-Synthesis Technique," M.S. Thesis, Polytechnic Univ. of Catalonia, Barcelona, Spain, 2010.

[15] Navarro Tapia, D., Marcos, A., Bennani, S., and Roux, C., "Joint Robust Structured Design of VEGA Launcher's Rigid-Body Controller and Bending Filter," *Proceedings of the 69th International Astronautical Congress*, Vol. 1, Curran Associates, Inc., IAC Paper :18-C1.5.3, Red Hook, NY, 2018, pp. 7980–7993.

[16] Wie, B., and Byun, K.-W., "New Generalized Structural Filtering Concept for Active Vibration Control Synthesis," *Journal of Guidance, Control, and Dynamics*, Vol. 12, No. 2, 1989, pp. 147–154. https://doi.org/10.2514/3.20384

[17] Zhai, W., Kelly, P., and Gong, W.-B., "Genetic Algorithms with Noisy Fitness," *Mathematical and Computer Modelling*, Vol. 23, Nos. 11–12, 1996, pp. 131–142. https://doi.org/10.1016/0895-7177(96)00068-4

[18] Mitchell, M., *An Introduction to Genetic Algorithms (Complex Adaptive Systems)*, MIT Press, Cambridge, MA, 1998, pp. 116–120.

[19] Lagarias, J. C., Reeds, J. A., Wright, M. H., and Wright, P. E., "Convergence Properties of the Nelder–Mead Simplex Method in Low Dimensions," *SIAM Journal on Optimization*, Vol. 9, No. 1, 1998, pp. 112–147. https://doi.org/10.1137/S1052623496303470

[20] Johnson, D., "Terrestrial Environment (Climatic) Criteria Guidelines for Use in Aerospace Vehicle Development. 2008 Revision," NASA TM 2008-215633, 2008.

[21] Simplcio, P., Bennani, S., Marcos, A., Roux, C., and Lefort, X., "Structured Singular-Value Analysis of the VEGA Launcher in Atmospheric Flight," *Journal of Guidance, Control, and Dynamics*, Vol. 39, No. 6, 2016, pp. 1342–1355. https://doi.org/10.2514/1.G000335